ECGI simulation with current dipole sources in Tank-Cage volume conductor model

1 Forward calculation

We used the following Tank-Cage volume cunductor model (see, Fig. 1):

- Tank surface triangulated with 1538 triangles (771 nodes) and
- Cage surface triangulated with 1200 triangles (602 nodes),

for potential calculation with boundary element method (BEM) and for calculating electrocardiographic imaging (ECGI) transfer matrix.

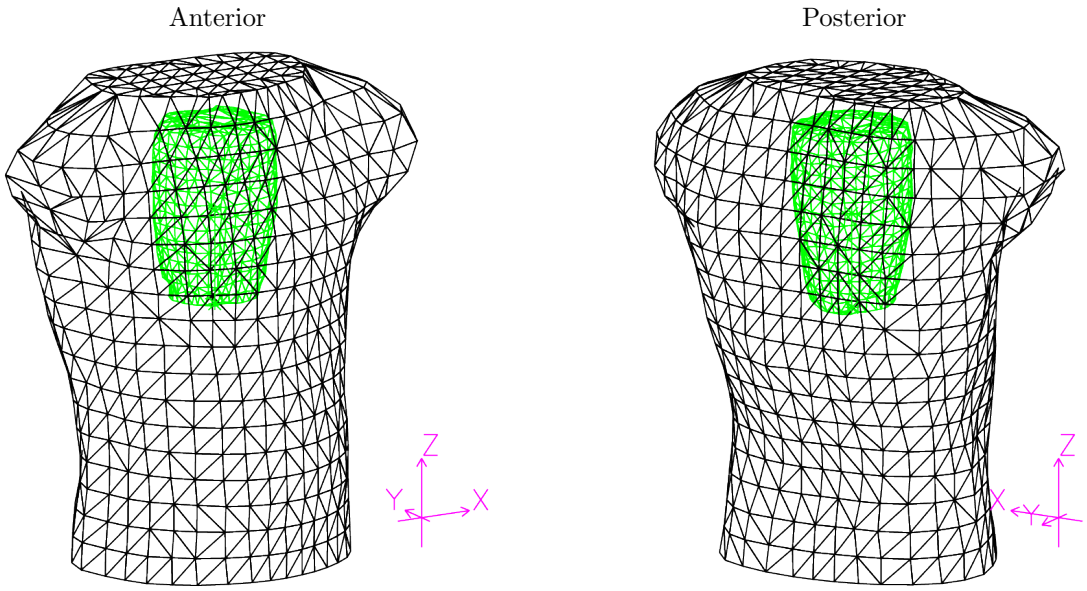

Fig. 1: BEM volume conductor model: Tank (black triangles) and cage (green triangles).

For this simulation, we created a cylindrical source space, consisted of 744 dipoles in 248 positions, which are arranged in 8 axial planes 10 mm apart along the z-axis. There are three perpendicular dipoles in each position: normal (radial) and tangential (along the polar angle) to the cage side surface, and alongside the polar z-axis. Fig. 2 shows cross-sectional views of the two BEM models and dipole positions on a given plane. In the first and second source (Axial) planes there are 7 source positions (Fig.2c), one in the center and 6 arranged along a concentric circle with radius 10 mm (nodes of hexagon with side 10 mm). Center of the bottom plane is at (-16,45,230) mm in the Cartesian coordinate system of the original Tank-Cage model. In the next two source planes (Fig. 2d), there are 19 positions on each plane, 7 like in the first and second planes and 12 arranged on an additional concentric circle with radius 20 mm (nodes of dodecagon with side 10 mm). In the next two source planes, there are 37 positions on each plane (Fig. 2e), 19 like in previous two planes and 18 on an additional concentric circle with radius 30 mm (nodes of octadecagon with side 10 mm). In the last two source planes, there are 61 positions on each plane (Fig. 2f), 37 like in the previous two planes and 24 on an additional concentric circle with radius 40 mm (nodes of tetracosagon with side 10 mm).

Each concentric circle represents a circumcircle of an equilateral polygon. The first node (dipole position) in a given circumcircle with radius ρ_i in the plane z_i is always in the most right side ($\varphi = \varphi_0 = -180$) in the cylindrical coordinate system of the source space. Next nodes have increasing polar angles in steps of $\Delta\varphi = 360/N_i$, where N_i is number of nodes (sides) of the equilateral polygon.

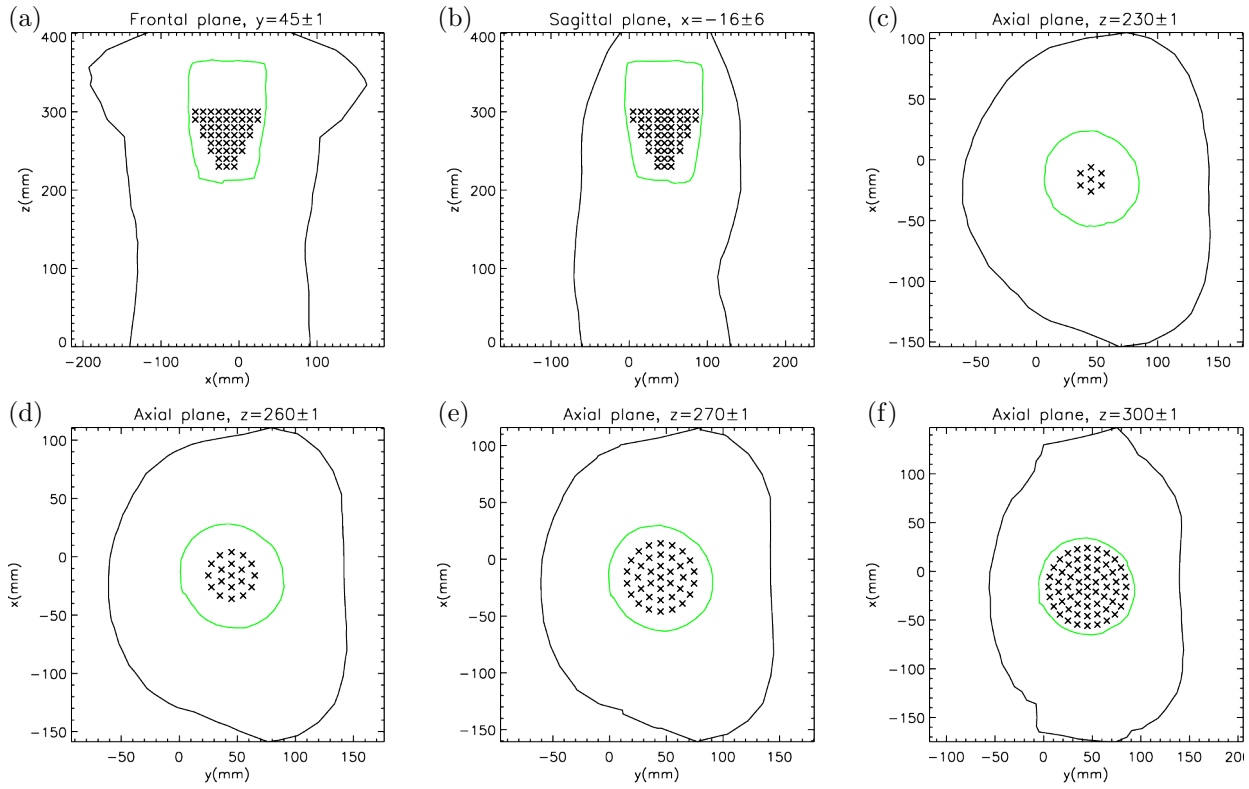

Fig. 2: Cross-sectional views of dipoles positions denoted by ×: a) Frontal, b) Sagittal and c)–f) Axial planes at different z levels. Tank and Cage borders are displayed with black and green colors, respectively. On each plane, sources within x or y or z levels ± tolerance are displayed. The polar axis of the cylindrical cage is at $x = -16\,\mathrm{mm}$ and $y = 45\,\mathrm{mm}$.

In each node, we put 3 dipoles pointing along coordinates in cylindrical coordinate system

- $\vec{p}_\rho = (1, 0, 0)$ – normal to the cage side surface
- $\vec{p}_\varphi = (0, 1, 0)$ – tangential to the cage side surface
- $\vec{p}_z = (0, 0, 1)$ – alongside the cage polar axis

Table 1 displays dipole numbering in different planes of the whole source space. Note, that the same enumeration is used also in calculated potential data.

Table 1: Dipole numbering in different source planes z - plane level, N_d - number of dipoles on a given plane and ρ - radial distance. On each plane, first three dipoles are positioned on the center (polar axis) and other in up to four concentric circles, where n is a total number of dipoles in a given circle, i_s and i_e are a starting and ending dipole number on that plane.

plane		Polar axis ($\rho = 0$)			1^{st} circle ($\rho = 10$)			2^{nd} circle ($\rho = 20$)			3^{rd} circle ($\rho = 30$)			4^{th} circle ($\rho = 40$)		
z	N_d	n	i_s	i_e	n	i_s	i_e	n	i_s	i_e	n	i_s	i_e	n	i_s	i_e
230	21	3	1	3	18	4	21									
240	21	3	22	24	18	25	42									
250	57	3	43	45	18	46	63	36	64	99						
260	57	3	100	102	18	103	120	36	121	156						
270	111	3	157	159	18	160	177	36	178	213	54	214	267			
280	111	3	268	270	18	271	288	36	289	324	54	325	378			
290	183	3	379	381	18	382	399	36	400	435	54	436	489	72	490	561
300	183	3	562	564	18	565	582	36	583	618	54	619	672	72	673	744
Σ	744	24			144			216			216			144		

2 Selection of sources

2.1 1-dipole

For 1-dipole source, we selected sources in four planes at levels(z_i): bottom plane ($z_1 = 230$), two planes in the middle ($z_2 = 260$ and $z_3 = 270$), and upper plane ($z_4 = 300$). On each plane, we selected four positions (in cylindrical coordinates ρ – radial distance, φ - polar angle, and z – height), one in the center (polar axis) and three on the outermost circle of a given plane:

$$\vec{r}_{i,1} = (0, 0, z_i),\ \vec{r}_{i,2} = (\rho_i, -180, z_i),\ \vec{r}_{i,3} = (\rho_i, -120, z_i),\ \vec{r}_{i,3} = (\rho_i, \varphi_i, z_i)\,, \tag{1}$$

where

$$\rho_1 = 10,\ \rho_2 = 20,\ \rho_3 = 30,\ \rho_4 = 40,\ \text{ and }\ \varphi_1 = -60,\ \varphi_2 = -90,\ \varphi_3 = -80,\ \varphi_4 = -75\,. \tag{2}$$

Table 2 shows positions of all selected dipoles and their numbers (n_ρ, n_φ, n_z) in the list of all 744 diploes source space. Altogether 12 dipoles are selected for each plane.

Table 2: Positions of all selected 1-dipole sources. (n_ρ, n_φ, n_z) are numbers of $\vec{p}_\rho$, $\vec{p}_\varphi$ and $\vec{p}_z$ dipoles in a given position.

plane	First position	Second position	Third position	Fourth position
z	(ρ,φ) , (n_ρ, n_φ, n_z)	(ρ, φ) , (n_ρ, n_φ, n_z)	(ρ, φ) , (n_ρ, n_φ, n_z)	(ρ, φ) , (n_ρ, n_φ, n_z)
230	(0,0) , (1, 2, 3)	(10,-180) , (4, 5, 6)	(10,-120) , (7, 8, 9)	(10,-60) , (10, 11, 12)
260	(0,0) , (100,101,102)	(20,-180) , (121,122,123)	(20,-120) , (127,128,129)	(20,-90) , (130,131,132)
270	(0,0) , (157,158,159)	(30,-180) , (214,215,216)	(30,-120) , (223,224,225)	(30,-80) , (229,230,231)
300	(0,0) , (562,563,564)	(40,-180) , (673,674,675)	(40,-120) , (685,686,687)	(40,-75) , (694,695,696)

Figure 3 displays positions of 1-dipole sources from Table 2. Potential maps of selected single dipole sources are displayed in a separated document *ECGI_simulation_1dipole_maps.pdf*

2.2 2-dipoles

For 2-dipoles sources, we selected single dipole sources in three planes at levels(z_i): two planes in the middle ($z_2 = 260$ and $z_3 = 270$), and upper plane ($z_4 = 300$). Note, that we kept the same notation of planes as in the case of 1-dipole sources. On each plane, we selected only dipoles in the outermost circle with radial distance ρ_i. We put the first single dipole on the right side (polar angle $\varphi = -180$). The other dipoles are then positioned in angular steps of $\Delta\varphi_i$ in the frontal part ($\varphi = -180 + \Delta\varphi_i,\ -180 + 2\Delta\varphi_i,\ \ldots, 0$). We combined dipoles along the same direction (3 parallel combinations: $(\vec{p}_\rho, \vec{p}_\rho)$, $(\vec{p}_\varphi, \vec{p}_\varphi)$, $(\vec{p}_z, \vec{p}_z)$ and 3 anti-parallel combinations: $(\vec{p}_\rho, -\vec{p}_\rho)$, $(\vec{p}_\varphi, -\vec{p}_\varphi)$, $(\vec{p}_z, -\vec{p}_z)$), as well as dipoles in different directions (6 orthogonal combinations: $(\vec{p}_\rho, \vec{p}_\varphi)$, $(\vec{p}_\rho, \vec{p}_z)$, $(\vec{p}_\varphi, \vec{p}_\rho)$, $(\vec{p}_\varphi, \vec{p}_z)$, $(\vec{p}_z, \vec{p}_\rho)$, $(\vec{p}_z, \vec{p}_\varphi)$). Table 3 shows positions and numbers of single dipoles used for 2-dipoles sources. For each direction $(\vec{p}_\rho, \vec{p}_\varphi, \vec{p}_z)$, there are N =6, 9 and 12 combinations of 2-dipoles positions in planes at levels z =260, 270 and 300, respectively.

All single dipoles have the same power ($p_i^2 = C$). In order to have the same source power also in the case of the 2-dipoles source, the potential of combined sources ($p_{\rm cmb}$) is calculated as a summation of the corresponding potential of single dipole sources (p_1 and p_2) divided by $\sqrt{2}$ ($p_{\rm cmb}^2 = p_1^2/2 + p_2^2/2 = C$).

Table 3: Positions ($(\varphi, \varphi = \varphi_0 + k\Delta\varphi, z)$, $k = 0, 1, \ldots, N$) and numbers $(n_\varphi, n_\varphi, n_z)$ of dipoles used for 2-dipoles sources.

plane	First dipoles	Other dipoles			
z , φ , $\Delta\varphi$	φ_0, (n_ρ, n_φ, n_z)	$\varphi_0 + \Delta\varphi$, (n_ρ, n_φ, n_z);	$\varphi + 2\Delta\varphi$, (n_ρ, n_φ, n_z);	$\ldots\ \varphi + N\Delta\varphi$, (n_ρ, n_φ, n_z)	N
260, 20, 30	-180, (121,122,123)	-150, (124,125,126);	-120, (127,128,129); ...	0, (139,140,141)	6
270, 30, 20	-180, (214,215,216)	-160, (217,218,219);	-140, (220,221,222); ...	0, (241,242,243)	9
300, 40, 15	-180, (673,674,675)	-165, (676,677,678);	-150, (679,680,681); ...	0, (709,710,711)	12

Figure 4 displays positions of 2-dipoles sources from Table 3. Potential maps of selected 2-dipoles sources are displayed in a separated document *ECGI_simulation_2dipole_maps.pdf*

2.3 3-dipoles

For 3-dipoles sources, we selected single dipole source positions that approximately form nodes of equilateral triangle. The first of the dipoles is in the center ($x = -16,\ y = 45$ in the Cartesiian coordinate of the original Tank & Cage model) of the bottom ($z = 230$) plane or some other planes in bottom part of the cage. The other two are positioned in the outermost circle of the upper ($z = 300$) or next but two ($z = 280$) source planes. We selected six triangles. Table 4 displays coordinates, single source numbers, distances between nodes and names of six selected triangles. Dipoles $(\vec{p}_\rho, \vec{p}_\varphi, \vec{p}_z)$ on each point are orthogonal to each other. One is approximately normal to the cage surface, and the other two are tangential. For the first triangle node, which is close to the cage bottom, the polar dipole with the opposite sign $(-\vec{p}_z)$ is normal to cage bottom, and for the other two nodes the radial $(\vec{p}_\rho)$ is normal to the cage side surface. For each triangle, we formed four 3-dipoles sources

1. normal with dipoles $(-\vec{p}_{1z}, \vec{p}_{2\rho}, \vec{p}_{3\rho})$
2. tangential with dipoles $(\vec{p}_{1\rho}, -\vec{p}_{2z}, \vec{p}_{3z})$
3. along the polar angle $(\vec{p}_{1\varphi}, \vec{p}_{2\varphi}, \vec{p}_{3\varphi})$, which are also all tangential to the cage side surface
4. axial with all dipoles along polar axis $(\vec{p}_{1z}, \vec{p}_{2z}, \vec{p}_{3z})$, which are also all perpendicular to the axial plane

Like in the case of the 2-dipoles sources, the potential of a combined source ($p_{\rm cmb}$) is calculated as a summation of the corresponding potential of single dipole sources (p_1, p_2 and p_3) divided by $\sqrt{3}$ in order to keep the same source power ($p^2_{\rm cmb} = p_1^2/3 + p_2^2/3 + p_3^2/3 = C$).

Table 4: Positions (ρ, φ, z) and numbers (n_ρ, n_φ, n_z) of dipoles used for 3-dipoles sources. We formed six different triangles, which are named according to either an approximate cross-sectional plane where triangle nodes are positioned (Frontal and Sagittal) or a part of the cage (tank) where most nodes are positioned (Right). We added to each name, an approximate mean value of distances between triangle nodes, which are denoted by (d_{12}, d_{13}, d_{23}).

Triangle	First dipoles	Second dipoles	Third dipoles	Distances
name	(ρ,φ, z), (n_ρ, n_φ, n_z)	(ρ, φ, z), (n_ρ, n_φ, n_z)	(ρ, φ, z), (n_ρ, n_φ, n_z)	(d_{12}, d_{13}, d_{23})
Frontal_80	(0, 0,230), (1, 2, 3)	(40,-180,300), (673,674,675)	(40, 0,300), (709,710,711)	(80.6,80.6,80.0)
Sagittal_80	(0, 0,230), (1, 2, 3)	(40, -90,300), (691,692,693)	(40, 90,300), (727,728,729)	(80.6,80.6,80.0)
Right_57	(0, 0,260), (103,104,105)	(40,-180,300), (673,674,675)	(40, -90,300), (691,692,693)	(56.6,56.6,56.6)
Frontal_60	(0, 0,230), (1, 2, 3)	(30,-180,280), (268,269,269)	(30, 0,300), (295,296,297)	(58.3,58.3,60.0)
Sagittal_60	(0, 0,230), (1, 2, 3)	(30,-100,280), (280,281,282)	(30, 0,300), (307,308,310)	(58.3,58.3,60.0)
Right_42	(0, 0,250), (43, 44, 45)	(30,-180,280), (268,269,269)	(30,-100,280), (280,281,282)	(42.4,42.4,42.4)

Figure 5 displays positions of 3-dipoles sources from Table 4.

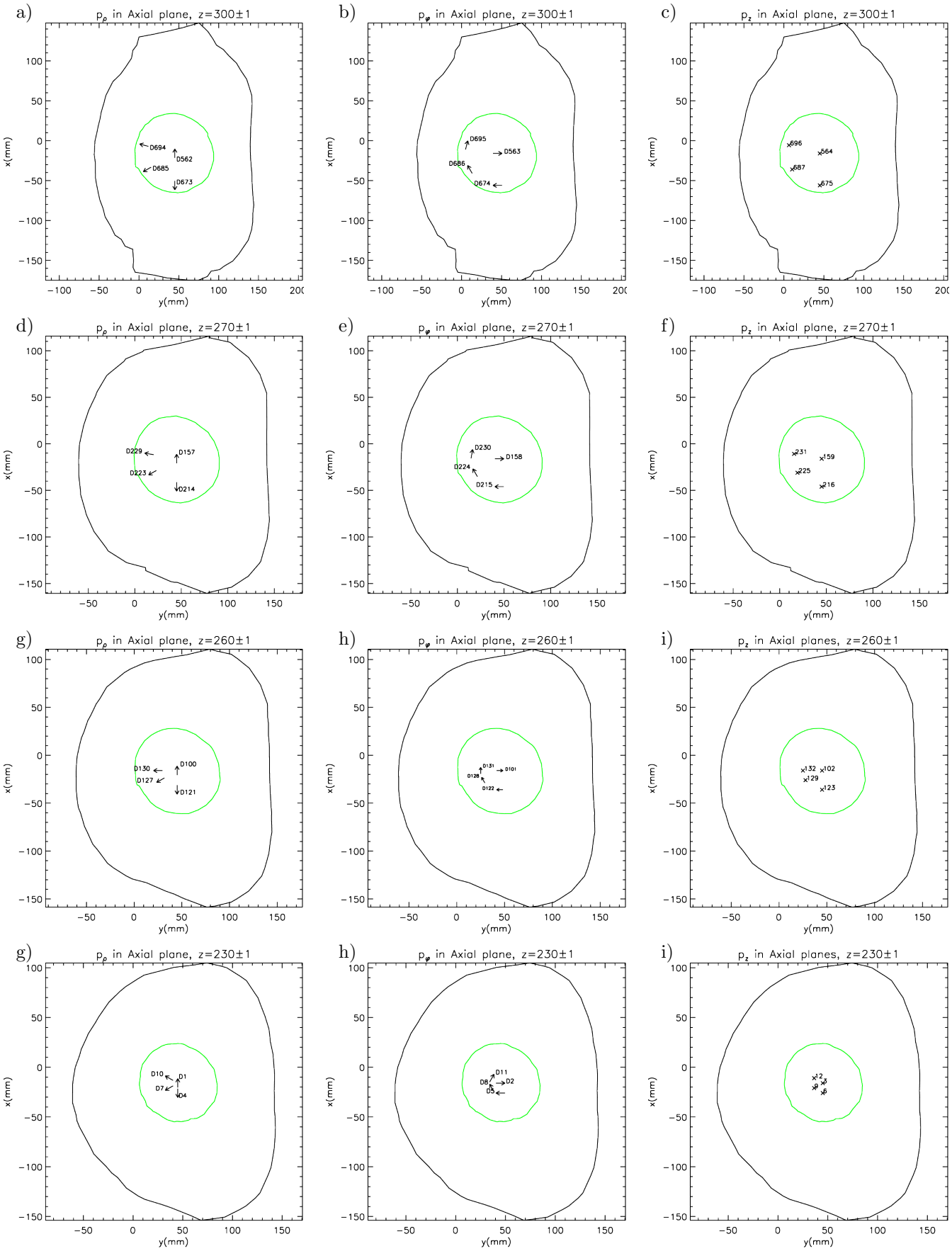

Fig. 3: Selected 1-dipole sources from Table 2. Labels denote dipole numbers in 744-dipoles source space (Fig. 2 and Table 1).

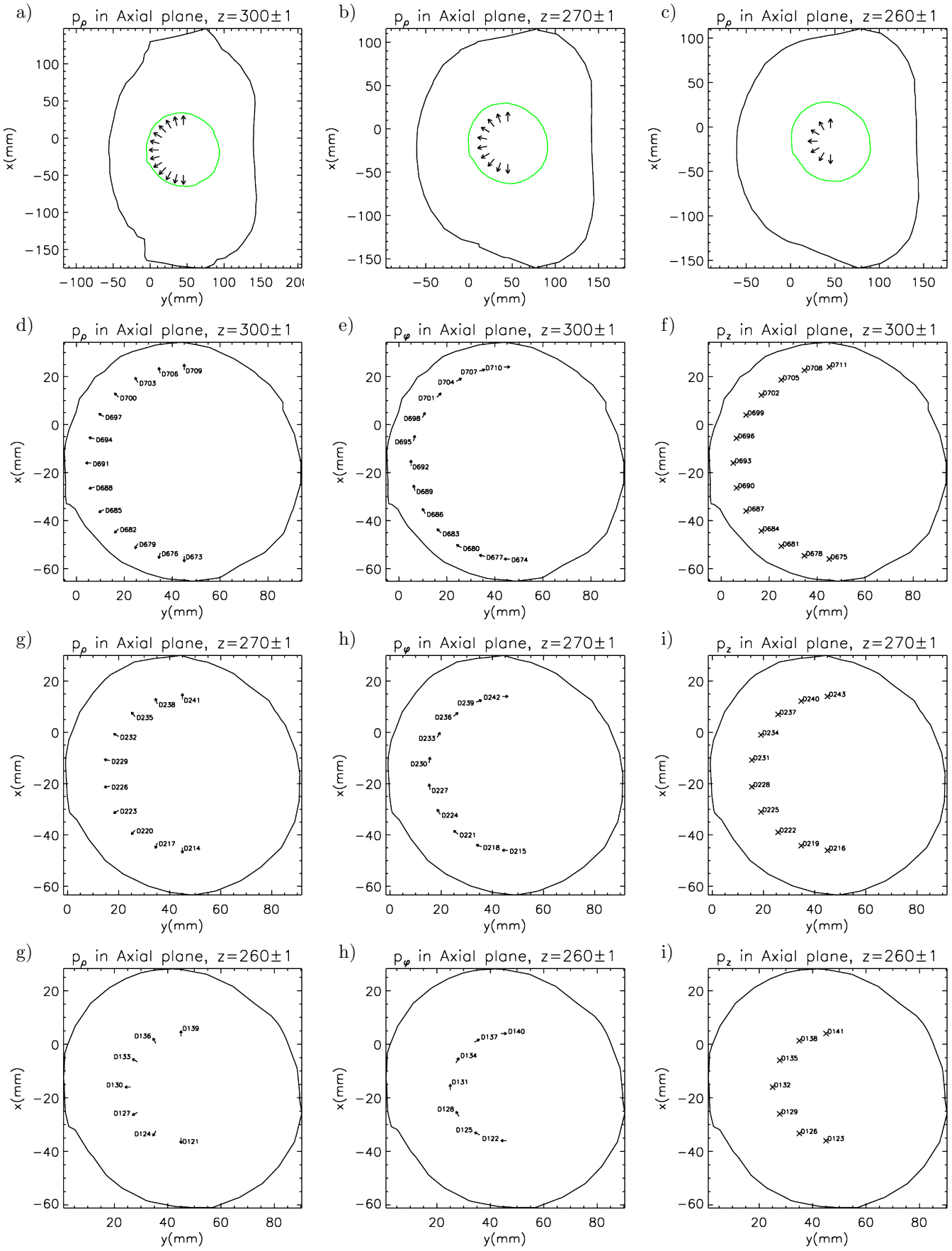

Fig. 4: Positions of 2-dipole sources (see, Table 3): a–c) radial dipoles in three axial planes z = 300, 270 and 260 mm, respectively, (torso border is displayed in black and cage border in green); d–i) labeled single dipoles used to construct 2-dipoles source models (only cage border is shown in black).

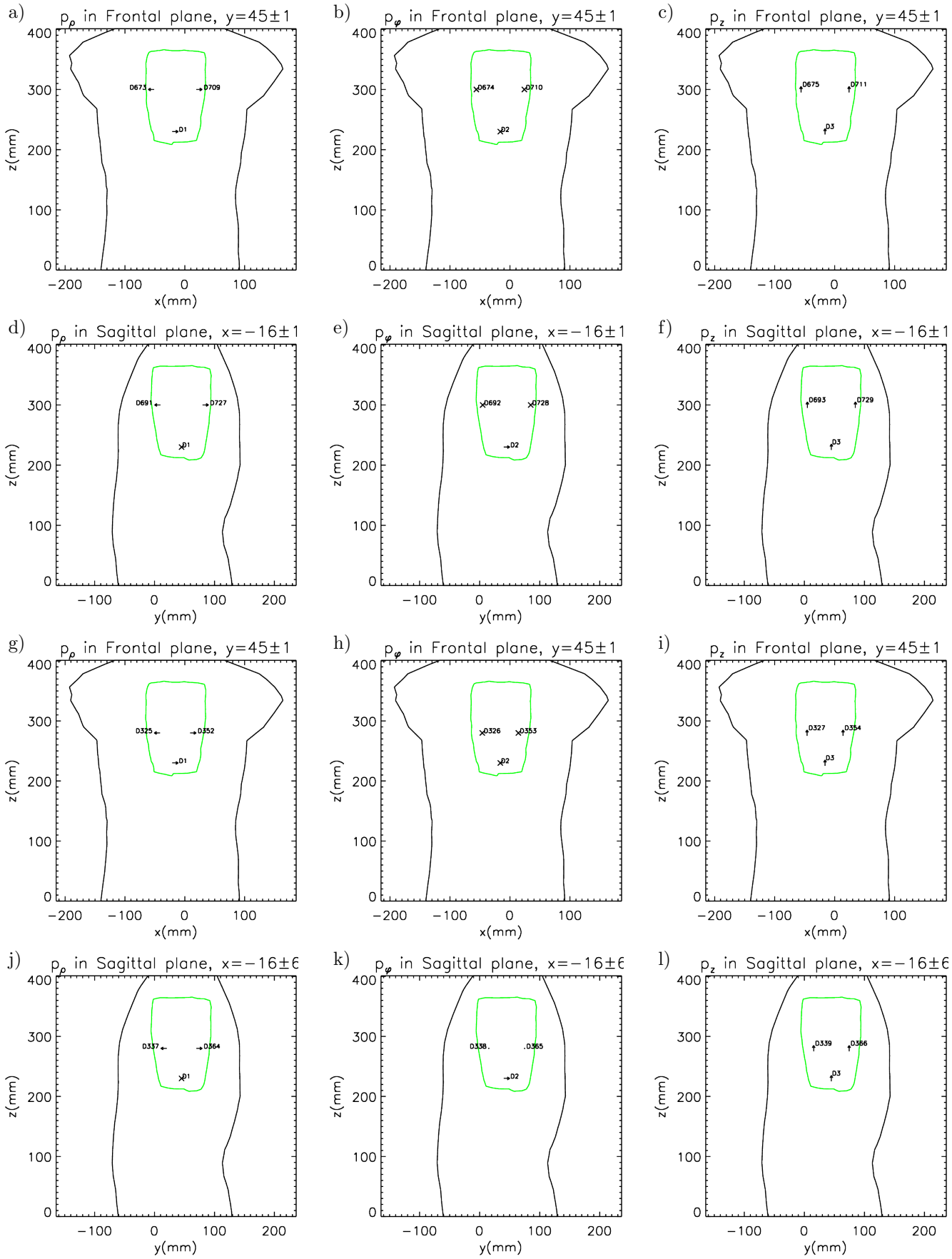

Fig. 5: Positions of 3-dipoles sources (see, Table 4): a-c) $(\vec{p}_\rho, \vec{p}_\varphi, \vec{p}_z)$-dipoles for Frontal_80, d-f) $(\vec{p}_\rho, \vec{p}_\varphi, \vec{p}_z)$-dipoles for Sagittal_80, g-i) $(\vec{p}_\rho, \vec{p}_\varphi, \vec{p}_z)$-dipoles for Frontal_60, and j-k) $(\vec{p}_\rho, \vec{p}_\varphi, \vec{p}_z)$-dipoles for Sagittal_50, respectively.